

Effect of the Synthesis Method of Chlorophyll-Ti₃C₂T_x Based Photocatalysts on Noble Metal-Free Hydrogen Evolution

Tianfang Zheng^a, Yuanlin Li^a, Yohan Dall'Agnese^b, Chunxiang Dall'Agnese^a, Shin-ichi Sasaki^{c,d}, Hitoshi Tamiaki^c and Xiao-Feng Wang^{a,*}

^a *Key Laboratory of Physics and Technology for Advanced Batteries (Ministry of Education), College of Physics, Jilin University, Changchun 130012, PR China*

^b *Institute for Materials Discovery, University College London, London WC1E 7JE, United Kingdom*

^c *Graduate School of Life Sciences, Ritsumeikan University, Kusatsu, Shiga 525-8577, Japan*

^d *Nagahama Institute of Bio-Science and Technology, Nagahama, Shiga 526-0829, Japan*

Abstract

Composites composed of chlorophyll and Ti₃C₂T_x MXene recently showed promising results as photocatalysts for hydrogen evolution reaction (HER). Herein, this type of composite is prepared by synthesizing the layered Ti₃C₂T_x material via an HCl@LiF etching technique, instead of the previously adopted HF etching technique. The performance of H₂ evolution, therefore, had a fourfold increase in our

photocatalytic system, in contrast to the one reported in the previous works. The underlying reason for such a large improvement of the chlorophyll-MXene photocatalyst performance is believed to be attributed to more suitable surface chemistry, higher conductivity, fewer defects, higher surface area, and larger interlayer space of $\text{Ti}_3\text{C}_2\text{T}_x$ introduced by the Li^+ ions from LiF in the etching process. Our work reveals that the synthesis method of MXenes used as the co-catalysts is key to improve the H_2 evolution efficiency in photocatalytic water splitting.

Introduction

It is well known that fossil fuel is a conventional but nonrenewable energy source. The immoderate utilization of fossil fuels is considered to cause serious environmental problems.¹⁻⁴ In this context, it is necessary to seek other emerging energy sources for sustainable development. Hydrogen is viewed as a promising alternative since its heat of combustion is three times higher than that of gasoline and other kinds of fossil fuels, and it can be used in hydrogen fuel cells. In addition, hydrogen is an environment-friendly fuel since its products after burning is clean. Meanwhile, in the context of the continuous decline of fossil fuels, solar energy has attracted tremendous attention as clean and renewable energy. The utilization of solar energy is mainly divided into photothermal conversion and photoelectric conversion. A case in point of these conversions is to produce hydrogen through photocatalytic water decomposition. To our knowledge, artificial photocatalysts can be classified into the following categories: (a) Molecular dye photocatalysts; (b) Traditional semiconductor-based photocatalysts;

(c) Quantum-dots-based photocatalyst; and (d) Two-dimensional material-based photocatalysts. In contrast with the traditional hydrogen production methods such as electrocatalytic water splitting hydrogen evolution reaction (HER) with noble metals as co-catalysts, photocatalysis technology for hydrogen production has the advantage of low electricity consumption and low cost due to the noble metal-free co-catalysts.⁵⁻¹¹

As one of the most common natural pigments, chlorophylls (Chls) exist in green plants and bacteria widely.¹² The role of Chls in natural photosynthesis is light capture and exciton transfer.¹³ Chl and its derivatives are often considered to be one of the best choices for photosensitizers because they are abundant and environmentally friendly. Due to the fascinating photochemical and photophysical properties of Chls, dye-sensitized solar cells with Chls and their derivatives as sensitizers are considered to be among the most potential candidates in the next generation of photovoltaic devices.^{12, 14-16} The special light trapping, electron/excited state migration, and hole back-transfer of Chls also provide a new mechanism for the inhibition of electron and hole recombination, which has a vital influence on the efficiency of photocatalytic hydrogen production reaction.

MXenes, for instance, $Ti_3C_2T_x$, as a new kind of two-dimensional(2D) layered materials, were firstly discovered in 2011.¹⁷ MXenes are synthesized through etching the A elements of MAX phases.^{18, 19} MAX phases are ternary carbides or nitrides with a $M_{n+1}AX_n$ formula, where $n = 1, 2, \text{ or } 3$, M is a transition metal element, A is an A-group element, X is carbon, and/or nitrogen.¹⁹ It is also demonstrated that $Ti_3C_2T_x$, a typical MXene, has excellent performance as a co-catalyst in photocatalytic water

splitting.^{4, 9, 20} To our knowledge, there are two most commonly used methods of etching to get $Ti_3C_2T_x$ from Ti_3AlC_2 in the literature.^{17, 18} One is to use aqueous HF to etch directly the Al layer of Ti_3AlC_2 , while the other is to add LiF into HCl to *in-situ* generate HF.¹⁸ So far, $Ti_3C_2T_x$ MXene as co-catalyst in photocatalytic water splitting HER was all synthesized through the first method, with various pigments as the main catalysts. For example, by using Chls as the main catalysts, it was reported by Li. et al that the highest H_2 production efficiency was about $20 \pm 2 \mu mol h^{-1} g^{-1}$.⁹ In contrast, the investigation with $Ti_3C_2T_x$ MXene synthesized by the second method in photocatalytic water splitting HER is still lacking. It was presumed that the two methods to fabricate $Ti_3C_2T_x$ give the same result about the co-catalyst performance because the two methods yield essentially the same material.

In the present work, we establish a new photocatalytic system for water splitting HER composed of Chl (see molecular structure in Supporting Information) as well as $Ti_3C_2T_x$ MXene which was etched by the HCl and LiF mixture method. Surprisingly, the efficiency reaches $86 \pm 2 \mu mol h^{-1} g^{-1}$, which is much higher than the result of Li. et al,⁹ where the co-catalyst $Ti_3C_2T_x$ MXene was synthesized by the HF etching method. This indicates that $Ti_3C_2T_x$ MXene obtained by the two methods has distinct co-catalysts performance and the HCl@LiF etching method can produce better co-catalysts performance. To explore the underlying reasons for such a difference, we employ the X-ray diffraction (XRD) and scanning electron microscope (SEM) to characterize the structure of $Ti_3C_2T_x$ MXene made by two different methods, as well as analyze known literature. Possible reasons can be synergistic effects linked with that

$\text{Ti}_3\text{C}_2\text{T}_x$ MXene obtained by the HCl@LiF method has a much larger interlayer space and surface area, higher conductivity, higher hydrophilicity, fewer defects, and different surface chemistry (more $-\text{OH}^-$ and less $-\text{F}^-$) than if obtained by HF method. This viewpoint can explain the better co-catalyst performance of the $\text{Ti}_3\text{C}_2\text{T}_x$ MXene by the second method. We also perform other experimental measurements such as electrochemical impedance spectra (EIS) and transient photocurrent (TPC), which further support our hypothesis. Our result demonstrates a new way to improve the hydrogen production efficiency in the $\text{Chl-Ti}_3\text{C}_2\text{T}_x$ catalysts system and encourage the fine-tuning of MXene.

2. Results and Discussion

For the convenience of comparison, hereafter multilayered $\text{Ti}_3\text{C}_2\text{T}_x$ MXene etched by HF or HCl@LiF are labeled HF- $\text{Ti}_3\text{C}_2\text{T}_x$ or $\text{HCl@LiF-Ti}_3\text{C}_2\text{T}_x$, respectively. The composite of Chl and $\text{Ti}_3\text{C}_2\text{T}_x$ etched directly by aqueous HF is labeled Chl/HF- $\text{Ti}_3\text{C}_2\text{T}_x$, while the composite of Chl and $\text{Ti}_3\text{C}_2\text{T}_x$ etched by HCl@LiF is labeled Chl/ $\text{HCl@LiF-Ti}_3\text{C}_2\text{T}_x$. Additionally, a contrast sample of delaminated $\text{Ti}_3\text{C}_2\text{T}_x$ was prepared and labeled d- $\text{Ti}_3\text{C}_2\text{T}_x$ and the composite of Chl and d- $\text{Ti}_3\text{C}_2\text{T}_x$ is labeled Chl/d- $\text{Ti}_3\text{C}_2\text{T}_x$.

2.1 Characterization of Structures and Morphology

Fig. 1a shows the XRD patterns of Ti_3AlC_2 MAX and $\text{Ti}_3\text{C}_2\text{T}_x$ MXenes obtained by the two distinct etching methods. For Ti_3AlC_2 , the most intense (103) peak at about 39° is characteristic of the MAX phase. After the etching process, this intense (103)

peak disappeared as well as (002) and (004) peaks downshifted, which means the complete transformation from the MAX phase to MXene. It's noteworthy that the 2θ of (002) peak of $\text{Ti}_3\text{C}_2\text{T}_x$ MXene etched by HCl@LiF moved from 9.4° to 5.3° , whereas that of $\text{Ti}_3\text{C}_2\text{T}_x$ MXene etched by aqueous HF moved leftward only to 7.8° , a relatively larger value than 5.3° . The c -lattice parameters can be calculated from the position of the (002) peak using Bragg's equation. The c -lattice parameters were found to be 33.49\AA and 22.65\AA for HCl@LiF and HF methods respectively. Similar to previously reported by Ghidui et al.²¹, the c -lattice parameters of $\text{Ti}_3\text{C}_2\text{T}_x$ etched by HCl@LiF is much higher than that of $\text{Ti}_3\text{C}_2\text{T}_x$ etched by HF. Assuming the $\text{Ti}_3\text{C}_2\text{T}_x$ layer thickness (approximately 1.6nm^{22}) is similar regardless of the synthesis method, such a phenomenon implies that $\text{Ti}_3\text{C}_2\text{T}_x$ MXene etched by HCl@LiF has a larger interlayer space than $\text{Ti}_3\text{C}_2\text{T}_x$ MXene etched by aqueous HF. After mixing with Chl, the peaks of Chl/HF- $\text{Ti}_3\text{C}_2\text{T}_x$ and Chl/ HCl@LiF - $\text{Ti}_3\text{C}_2\text{T}_x$ all shifted downwards, which indicated that Chl has been successfully inserted into the interlayer space of $\text{Ti}_3\text{C}_2\text{T}_x$ (Fig. S2).

Fig. 1b shows the fluorescence spectra of the two composites used in HER tests. To make a comparison, the spectrum of pure Chl is also shown. We found that the emission peaks of the three samples occur at almost the same position with a wavelength of 660 nm. Due to the autogenic recombination of the photogenerated electron-hole pairs, it is reasonable that the pristine Chl has the strongest peak. As for the two composites, the $\text{Ti}_3\text{C}_2\text{T}_x$ MXene affects inhibition of the recombination of photogenerated electron-hole pairs due to the electron transfer from Chl to $\text{Ti}_3\text{C}_2\text{T}_x$. Consequently, the peaks of the two composites both have relatively lower intensity, in

comparison with that of the pristine Chl. Moreover, it can be found that the emission peak of Chl/HCl@LiF- $\text{Ti}_3\text{C}_2\text{T}_x$ is less intensive than Chl/HF- $\text{Ti}_3\text{C}_2\text{T}_x$, which indicates that the inhibition effect on the recombination of photogenerated electron-hole pairs is more effective in Chl/HCl@LiF- $\text{Ti}_3\text{C}_2\text{T}_x$.

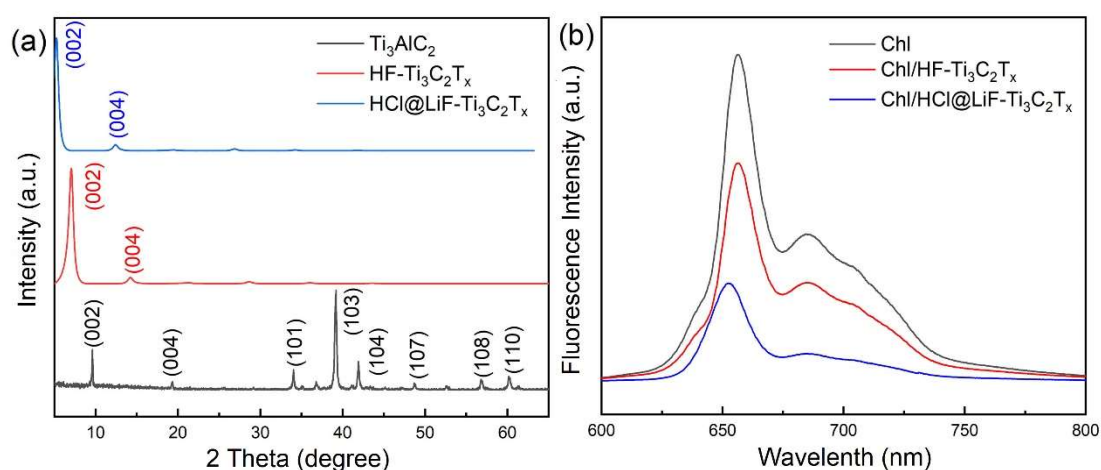


Fig.1 (a) XRD patterns of Ti_3AlC_2 MAX phase and $\text{Ti}_3\text{C}_2\text{T}_x$ samples used in HER tests;
(b) Fluorescence spectra of the composites as well as Chl pristine.

Fig. 2 shows the SEM images of the $\text{Ti}_3\text{C}_2\text{T}_x$ samples in various circumstances. It can be found that the etched $\text{Ti}_3\text{C}_2\text{T}_x$ sample shown in Fig. 2a has a relatively larger interlayer space than in Fig. 2b. Similarly, the interlayer space of composite Chl/HCl@LiF- $\text{Ti}_3\text{C}_2\text{T}_x$ shown in Fig. 2c is larger than that of composite Chl/HF- $\text{Ti}_3\text{C}_2\text{T}_x$ shown in Fig. 2d. In addition, we have to point out that due to the small molecular aggregation on $\text{Ti}_3\text{C}_2\text{T}_x$ instead of a large molecular aggregation produced by Chl, the Chl deposited on $\text{Ti}_3\text{C}_2\text{T}_x$ is difficult to observe. As shown in Fig. 2, the $\text{Ti}_3\text{C}_2\text{T}_x$ and the composites all have a typical 2D nanosheet accordion-like structure, similar to graphene nanoplatelets. Usually, the utilization of the HCl@LiF etching method is to easily obtain delaminated $\text{Ti}_3\text{C}_2\text{T}_x$ MXene, but herein to provide a fair

comparison with the multilayered $Ti_3C_2T_x$ prepared by the HF method, we also focus the comparison on multilayered $HCl@LiF-Ti_3C_2T_x$ instead of delaminated ones.

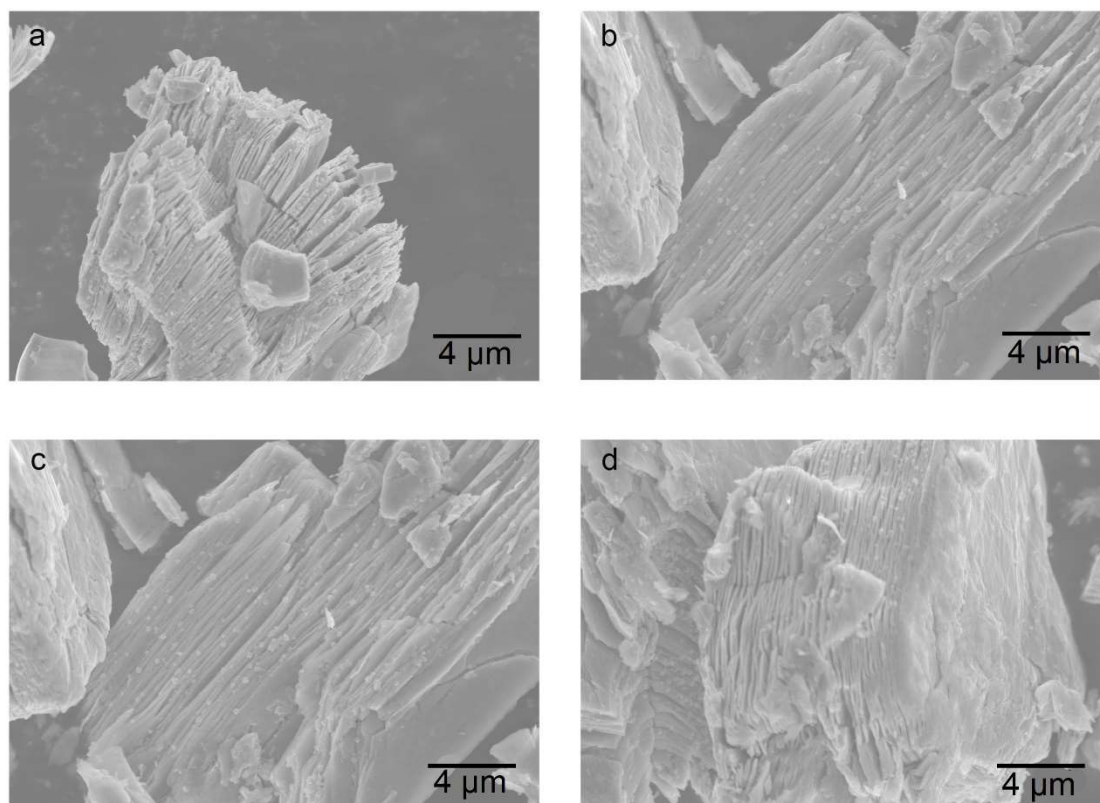


Fig.2 SEM images of (a) $HCl@LiF-Ti_3C_2T_x$; (b) $HF-Ti_3C_2T_x$; (c) $Chl/HCl@LiF-Ti_3C_2T_x$; (d) $Chl/HF-Ti_3C_2T_x$.

Additionally, the specific surface area (SSA) of the samples was measured by nitrogen gas sorption and calculated using the BET method (Table S1). For reference, we have also synthesized a control group of catalyst system with Chl and d- $Ti_3C_2T_x$ MXene (see XRD pattern and SEM image of d- $Ti_3C_2T_x$ in Supporting Information), the HER result and specific surface area (SSA) of the control group have also been tested to discuss whether the SSA of $Ti_3C_2T_x$ MXene is the key point of the better co-catalysts performance. The SSA of $Chl/HF-Ti_3C_2T_x$, $Chl/HCl@LiF-Ti_3C_2T_x$, $Chl/d-Ti_3C_2T_x$ were found to be 5.5, 9.6, and 12.1 m^2g^{-1} . Thus, the difference between $Chl/HF-Ti_3C_2T_x$

and Chl/HCl@LiF-Ti₃C₂T_x is too similar to be significant, considering the order of experimental error. These two composites can be considered to have approximately the same SSA, thus the difference in the performance in catalysis must be explained by other reasons, such as defect and surface chemistry.

To our knowledge, the HCl@LiF etching method improve the product quality, which means it causes fewer defects²¹. The fewer defects cause fewer electron scatterings, thus improve the conductivity, which can directly improve the conductivity of Ti₃C₂T_x MXene, and improve the co-photocatalytic performance. Besides, the different etching methods also result in different surface chemistry. The HCl@LiF etching method will introduce more -OH terminations and less -F terminations, which can also improve the HER results.²⁰

2.2 Photoelectrochemical Performance

To further investigate the improved co-catalyst performance of Ti₃C₂T_x etched by HCl@LiF, the photoelectrochemical behaviors of composites Chl/HCl@LiF Ti₃C₂T_x and Chl/HF- Ti₃C₂T_x have been measured through EIS and TPC tests, as displayed in Fig. 3.

The inset of Fig. 3a is a fitting circuit to simulate the EIS test, where R₁ represents the resistance of the electrolyte solution, and R₂ represents the interfacial charge transfer resistance between electrode and electrolyte. The constant phase element is indicated as CPE, and W₀ stands for the Warburg impedance. The diameter of the major semi-circle reflects the resistance of electron transfer between Chl and Ti₃C₂T_x. A

smaller radius means a more remarkable spatial separation efficiency of photogenerated electron-hole pairs. The radius of the semi-circle of Chl/HCl@LiF- $\text{Ti}_3\text{C}_2\text{T}_x$ in the EIS spectra is obviously smaller than that of Chl/HF- $\text{Ti}_3\text{C}_2\text{T}_x$, implying that the electron transfer from Chl to $\text{Ti}_3\text{C}_2\text{T}_x$ in Chl/HCl@LiF- $\text{Ti}_3\text{C}_2\text{T}_x$ is much easier than that in Chl/HF- $\text{Ti}_3\text{C}_2\text{T}_x$. This result indicates the more efficient separation of photogenerated electron-hole pairs in Chl/HCl@LiF- $\text{Ti}_3\text{C}_2\text{T}_x$, which would be advantageous for photocatalytic performance.

The results of the TPC test are shown in Fig. 3b. When being illuminated, both of the composites Chl/HCl@LiF- $\text{Ti}_3\text{C}_2\text{T}_x$ and Chl/HF- $\text{Ti}_3\text{C}_2\text{T}_x$ show rapid current rise responses. The response is a signal of the separation of the photogenerated electron-hole pairs due to the electron transfer from Chl to $\text{Ti}_3\text{C}_2\text{T}_x$. It also shows the photocurrent response of composite Chl/HCl@LiF- $\text{Ti}_3\text{C}_2\text{T}_x$ is stronger. This is consistent with the EIS results. Therefore, based on EIS and TPC results, we can conclude that with the same Chl as the photocatalyst, HCl@LiF- $\text{Ti}_3\text{C}_2\text{T}_x$ can promote the separation of photogenerated electron-hole pairs, as a result, improving the photocatalytic performance.

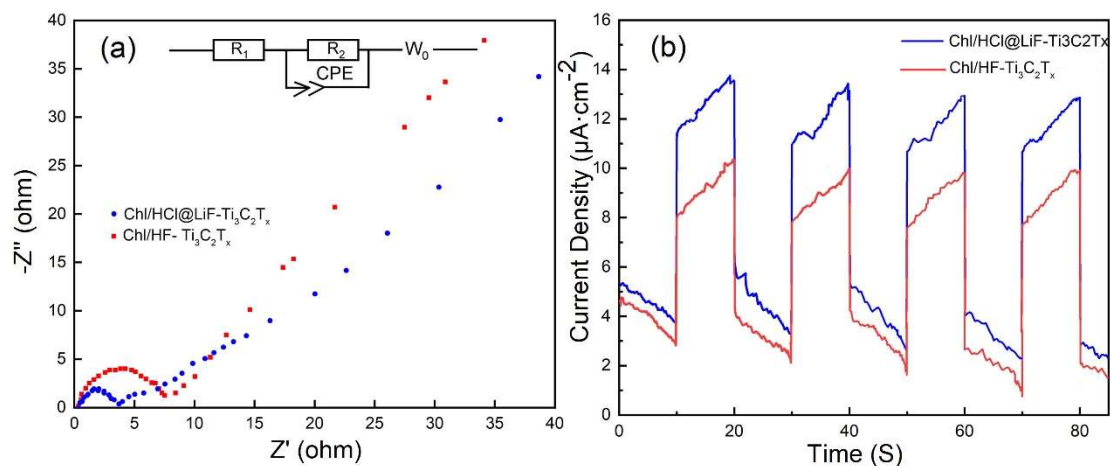


Fig.3 (a) EIS spectra of the two catalytic systems, and a fitting circuit of the EIS test illustrated in the inset; (b) Photocurrent responses of the two catalytic systems

From the results of EIS and TPC tests, we can draw a conclusion that the composite of Chl/HCl@LiF-Ti₃C₂T_x has better conductivity. The fact that Ti₃C₂T_x MXenes etched by HCl and LiF has better conductivity has been reported and proved in previous reports^{17, 21}, which might be a reason for the better co-photocatalytic performance herein we report.

2.3 Photocatalytic Performance

A comparison of the performance of photocatalytic water splitting HER under visible-to-near infrared light ($\lambda > 400$ nm) illumination for 6 hours is made between the composites Chl/HCl@LiF-Ti₃C₂T_x and Chl/HF-Ti₃C₂T_x. The photocatalytic performance is characterized by the efficiency of H₂ production, as shown in Fig. 3. Composite Chl/HF-Ti₃C₂T_x here showed an H₂ production efficiency of 18 $\mu\text{mol h}^{-1} \text{g}^{-1}$, which is roughly the same as that reported previously by Li. et al. What we would like to emphasize is that Chl/HCl@LiF-Ti₃C₂T_x is more efficient than the Chl/HF-Ti₃C₂T_x throughout the entire HER process. The efficiency of Chl/HCl@LiF-Ti₃C₂T_x reached 87 $\mu\text{mol h}^{-1} \text{g}^{-1}$, which is about four to five times higher than that of Chl/HF-Ti₃C₂T_x. For reference, the result of the HER test of the control group (Chl/d-Ti₃C₂T_x) was also included in Fig.3.

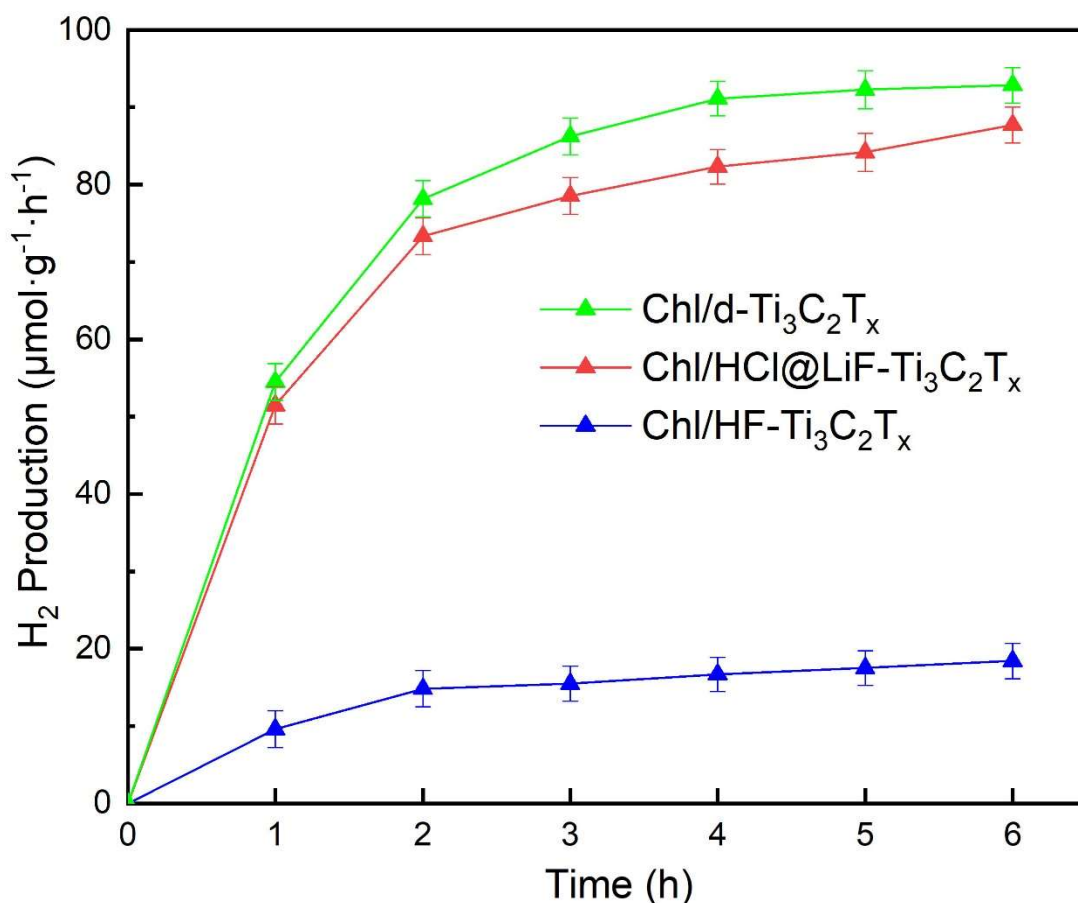


Fig.4 H₂ production performance of the three catalytic systems. The vertical bars stand for the fluctuations of experimental results.

2.4 Photocatalytic Mechanism

Due to its good conductivity, Ti₃C₂T_x is considered as the electrons sink in our system. A Schottky junction with a high potential barrier is formed between Chl and Ti₃C₂T_x. Upon illumination, Chl is excited and electron-hole pairs are generated. Then, the electron in the lowest unoccupied molecular orbital (LUMO) of Chl move towards Ti₃C₂T_x by passing through the Schottky junction. The hole that remained in Chl can be reduced by accepting an electron from the sacrificial reagent. Finally, the

transformed electrons in $Ti_3C_2T_x$ are captured by H^+ ions, hence H_2 is produced. In short, the hydrogen evolution reaction here can be summarized according to the above explanation as follows:



3. Conclusion

In summary, we synthesized a new composite of chlorophyll and $Ti_3C_2T_x$ MXene as a photocatalytic for HER, where $Ti_3C_2T_x$ MXene was prepared by the HCl@LiF etching technique. In comparison with a previous work where the nominally equal photocatalytic system was adopted but with $Ti_3C_2T_x$ MXene synthesized by HF etching, we find that our catalytic system can improve the H_2 production efficiency by about four to five times. After the characterization of the samples used in HER tests as well as analyzing the known literature, we put forward several possible reasons for better photocatalytic performance for our systems, such as a larger interlayer distance, higher conductivity, different surface chemistry, and fewer defects caused by HCl@LiF etching method of $Ti_3C_2T_x$ MXene. Our work demonstrates a new way to improve the hydrogen production efficiency in Chl/MXene catalysts systems and made a successful attempt of made adjustments to $Ti_3C_2T_x$ MXenes.

4. Experimental Section

Synthesis of Chl and $Ti_3C_2T_x$ MXenes: The synthesis of Chl was referred to

previous work. For the synthesis of $Ti_3C_2T_x$ MXene, the HF etching method was used, 1 g Ti_3AlC_2 MAX (Forsman, 98%) was slowly added into 49% HF, the solution was stirred at 350 rpm at room temperature for 24 h. By washing with the deionized water, the pH value of the solution reached almost 7, then the sediment was dried in a vacuum oven for 12 hours at 60°C. Another way of etching is the HCl@LiF method, 1,6 g LiF was slowly added into 20ml 6M HCl solution, and the mixture was stirred at 350 rpm for 5 min. 1 g Ti_3AlC_2 MAX (Forsman, 98%) was slowly into the mixture. The solution was stirred at 350 rpm at 35°C for 24 h. After that, the obtained solution was washed through centrifugation in deionized water till the pH value reached the neutral state, the neutral state mixture was freeze-dried in a vacuum environment to obtain $Ti_3C_2T_x$ MXene powder. For the synthesizing of d- $Ti_3C_2T_x$, the previous steps are the same as synthesizing normal multilayer LiF@HCl- $Ti_3C_2T_x$, then when the neutral solution of $Ti_3C_2T_x$ was obtained, the solution was put in an ultrasonic bath for 15 min and was centrifuged at 3000 rpm for 1 h. The obtained solution containing dark-green d- $Ti_3C_2T_x$ then was freeze-dried in a vacuum environment to obtain d- $Ti_3C_2T_x$ powder.

Synthesis of the Chl/ $Ti_3C_2T_x$ Composites: 3 mg $Ti_3C_2T_x$ MXene prepared by different etchants was put into two containers respectively. The mass ratio of Chl and $Ti_3C_2T_x$ was selected to be 6%. Chl was dissolved in tetrahydrofuran (THF) to obtain the solution with a concentration of 1 mg/ml. After that, 180 μ l obtained solution was added into the $Ti_3C_2T_x$ container. The mixture was stirred at 350 rpm at room temperature for 12 hours. After evaporation of THF in the glove box, the remaining solid was obtained as the resulting composite.

Characterization: To determine the differences in the structures of $\text{Ti}_3\text{C}_2\text{T}_x$ MXene synthesized by different methods, X-ray diffraction patterns were measured with a Cu $K\alpha$ radiation (Bruker D8). In addition, a scanning electron microscope (Hitachi, Regulus 8100 SEM) was used to observe the different microstructures of $\text{Ti}_3\text{C}_2\text{T}_x$ MXene synthesized by different methods. For the fluorescence test, a fluorospectrophotometer (Shimadzu, RF-6000) was used. 1 mg samples were dissolved in THF and were added into cuvette respectively. The solution was then illuminated with a wavelength of 436 nm, and the fluorescence intensity was measured by a fluorospectrophotometer.

Photocatalytic Activity Measurements: To measure the H_2 evolution efficiency in the HER, a 350 W xenon lamp (PLS-SXE300+, Perfectlight) ($\lambda > 400$ nm) with the light intensity of 80 mW/cm^2 was employed. The composites of $\text{ChI/Ti}_3\text{C}_2\text{T}_x$ were dispersed in a 3 ml aqueous solution with 55 mM ascorbic acid as a sacrificial reagent. The mixture was put into a 6 ml photoreactor and then stirred over 6 hours under illumination to avoid the presence of sediment. Before the measurement, the photoreactor containing solution was continuously purged with argon for 15 minutes to remove soluble oxygen. H_2 evolution was measured with the utilization of gas chromatography (SP-3420A, Beifen-Ruili, China).

Photochemical Performance: EIS test measurements were carried out with a three-electrode system by an electrochemical workstation (Bio-Logic SAS). The working electrode was $\text{ChI/Ti}_3\text{C}_2\text{T}_x$ composite on fluorine-doped tin oxide, the reference electrode was Ag/AgCl and the counter electrode was Pt plate. The solution

in the EIS tests was 0.5 M Na₂SO₄ aqueous solution with 2 g L⁻¹ AA. The measurement is in the range of 0.1 Hz to 100 kHz. For the TPC response, the same three-electrode system was utilized. A 350 W xenon lamp (PLS-SXE300+, Perfectlight) ($\lambda > 400$ nm) was utilized as the light source. All the measurements were conducted at room temperature.

1. Clarizia, L.; Russo, D.; Di Somma, I.; Andreozzi, R.; Marotta, R., Hydrogen Generation through Solar Photocatalytic Processes: A Review of the Configuration and the Properties of Effective Metal-Based Semiconductor Nanomaterials. *Energies* **2017**, *10*(10), 21.
2. Guo, Z. L.; Zhou, J.; Zhu, L. G.; Sun, Z. M., MXene: a promising photocatalyst for water splitting. *Journal of Materials Chemistry A* **2016**, *4* (29), 11446-11452.
3. Liu, Q. X.; Ai, L. H.; Jiang, J., MXene-derived TiO₂@C/g-C₃N₄ heterojunctions for highly efficient nitrogen photofixation. *Journal of Materials Chemistry A* **2018**, *6* (9), 4102-4110.
4. Lu, X. L.; Xu, K.; Chen, P. Z.; Jia, K. C.; Liu, S.; Wu, C. Z., Facile one step method realizing scalable production of g-C₃N₄ nanosheets and study of their photocatalytic H₂ evolution activity. *Journal of Materials Chemistry A* **2014**, *2* (44), 18924-18928.
5. Su, T. M.; Shao, Q.; Qin, Z. Z.; Guo, Z. H.; Wu, Z. L., Role of Interfaces in Two-Dimensional Photocatalyst for Water Splitting. *ACS Catal.* **2018**, *8* (3), 2253-2276.
6. Sun, Y.; Sun, Y.; Dall'Agnese, C.; Wang, X.-F.; Chen, G.; Kitao, O.; Tamiaki, H.; Sakai, K.; Ikeuchi, T.; Sasaki, S.-i., Dyad Sensitizer of Chlorophyll with Indoline Dye for Panchromatic Photocatalytic Hydrogen Evolution. *Acs Applied Energy Materials* **2018**, *1* (6), 2813-2820.
7. Xiang, Q. J.; Yu, J. G.; Jaroniec, M., Synergetic Effect of MoS₂ and Graphene as Cocatalysts for Enhanced Photocatalytic H₂ Production Activity of TiO₂ Nanoparticles. *J. Am. Chem. Soc.* **2012**, *134* (15), 6575-6578.
8. Zhu, J.; Ha, E. N.; Zhao, G. L.; Zhou, Y.; Huang, D. S.; Yue, G. Z.; Hu, L. S.; Sun, N.; Wang, Y.; Lee, L. Y. S.; Xu, C.; Wong, K. Y.; Astruc, D.; Zhao, P. X., Recent advance in MXenes: A promising 2D material for catalysis, sensor and chemical adsorption. *Coord. Chem. Rev.* **2017**, *352*, 306-327.
9. Li, Y.; Chen, X.; Sun, Y.; Meng, X.; Dall'Agnese, Y.; Chen, G.; Dall'Agnese, C.; Ren, H.; Sasaki, S.-i.; Tamiaki, H.; Wang, X.-F., Chlorosome-Like Molecular Aggregation of Chlorophyll Derivative on Ti₃C₂T_x MXene Nanosheets for Efficient Noble Metal-Free Photocatalytic Hydrogen Evolution. *Advanced Materials Interfaces* **2020**, *7*(8).
10. Sun, Y.; Sun, Y.; Meng, X.; Gao, Y.; Dall'Agnese, Y.; Chen, G.; Dall'Agnese, C.; Wang, X.-F., Eosin Y-sensitized partially oxidized Ti₃C₂ MXene for photocatalytic hydrogen evolution. *Catalysis Science & Technology* **2019**, *9*(2), 310-315.
11. Sun, Y.; Sun, Y. L.; Dall'Agnese, C.; Wang, X. F.; Chen, G.; Kitao, O.; Tamiaki, H.;

- Sakai, K.; Ikeuchi, T.; Sasaki, S., Dyad Sensitizer of Chlorophyll with Indoline Dye for Panchromatic Photocatalytic Hydrogen Evolution. *Acs Applied Energy Materials* **2018**, *1* (6), 2813-2820.
12. Wang, X.-F.; Kitao, O.; Zhou, H.; Tamiaki, H.; Sasaki, S.-i., Efficient Dye-Sensitized Solar Cell Based on oxo-Bacteriochlorin Sensitizers with Broadband Absorption Capability. *Journal of Physical Chemistry C* **2009**, *113* (18), 7954-7961.
13. Tamiaki, H.; Shibata, R.; Mizoguchi, T., The 17-propionate function of (bacterio)chlorophylls: Biological implication of their long esterifying chains in photosynthetic systems. *Photochemistry and Photobiology* **2007**, *83* (1), 152-162.
14. Wang, X.-F.; Tamiaki, H.; Kitao, O.; Ikeuchi, T.; Sasaki, S.-i., Molecular engineering on a chlorophyll derivative, chlorin e(6), for significantly improved power conversion efficiency in dye-sensitized solar cells. *Journal of Power Sources* **2013**, *242*, 860-864.
15. Wang, X. F.; Kitao, O., Natural Chlorophyll-Related Porphyrins and Chlorins for Dye-Sensitized Solar Cells. *Molecules* **2012**, *17* (4), 4484-4497.
16. Xu, W.; Zhao, X.; Tang, J.; Zhang, C.; Gao, Y.; Sasaki, S.-i.; Tamiaki, H.; Li, A.; Wang, X.-F., Synthesis of Chl@Ti₃C₂ composites as an anode material for lithium storage. *Frontiers of Chemical Science and Engineering* **2020**.
17. Alhabeab, M.; Maleski, K.; Anasori, B.; Lelyukh, P.; Clark, L.; Sin, S.; Gogotsi, Y., Guidelines for Synthesis and Processing of Two-Dimensional Titanium Carbide (Ti₃C₂TX MXene). *Chem. Mat.* **2017**, *29* (18), 7633-7644.
18. Alhabeab, M.; Maleski, K.; Mathis, T. S.; Sarycheva, A.; Hatter, C. B.; Uzun, S.; Levitt, A.; Gogotsi, Y., Selective Etching of Silicon from Ti₃SiC₂ (MAX) To Obtain 2D Titanium Carbide (MXene). *Angew. Chem.-Int. Edit.* **2018**, *57* (19), 5444-5448.
19. Naguib, M.; Mochalin, V. N.; Barsoum, M. W.; Gogotsi, Y., 25th Anniversary Article: MXenes: A New Family of Two-Dimensional Materials. *Adv. Mater.* **2014**, *26* (7), 992-1005.
20. Sun, Y.; Jin, D.; Sun, Y.; Meng, X.; Gao, Y.; Dall'Agnese, Y.; Chen, G.; Wang, X.-F., g-C₃N₄/Ti₃C₂T_x (MXenes) composite with oxidized surface groups for efficient photocatalytic hydrogen evolution. *Journal of Materials Chemistry A* **2018**, *6* (19), 9124-9131.
21. Ghidui, M.; Lukatskaya, M. R.; Zhao, M. Q.; Gogotsi, Y.; Barsoum, M. W., Conductive two-dimensional titanium carbide 'clay' with high volumetric capacitance. *Nature* **2014**, *516* (7529), 78-U171.
22. Lipatov, A.; Lu, H. D.; Alhabeab, M.; Anasori, B.; Gruverman, A.; Gogotsi, Y.; Sinitskii, A., Elastic properties of 2D Ti₃C₂T_x MXene monolayers and bilayers. *Sci. Adv.* **2018**, *4* (6), 7.